June 14, 2006

Specifications of the GASE Antennas

Paul S. Ray[1], Kenneth P. Stewart, Brian C. Hicks, Emil J. Polisensky (NRL)

1. Introduction

In this document we describe the antennas deployed as part of the initial GRB All-sky Spectroscopic Experiment (GASE) array Morales et al. (2006). The scientific goals of GASE require sky-noise-limited performance in the 30–40 MHz range and as broad a response pattern as possible. Because of the limited budget, a custom design and fabrication of antennas was not feasible, so we chose to use a slight modification of a prototype antenna and active balun being designed and built for the Long Wavelength Array project.

2. Physical Specifications

The GASE dipoles are constructed out of 3/8 inch diameter copper pipe and standard pipe fittings silver soldered together. The masts are made of UV-resistant fiberglass. The dimensions of the antenna are shown in Figure 1, and a photo of an antenna installed in the field is shown in Figure 2.

3. Electrical Properties

The RF properties of the antenna were simulated using EZNEC/4 (http://www.eznec.com) and the results are described in the following sections. The simulations were done assuming that the antenna material is 3/8 inch diameter copper tubing with resistivity $\rho = 1.74 \times 10^{-8}$ Ω-m. The antenna was placed over a simulated infinite ground plane with typical properties (conductivity $\sigma = 0.005$ S/m and dielectric constant $\epsilon = 13$).

The simulation was done using the input file shown in Listing 1. The definitions of the input cards can be found at http://www.nec2.org/part_3/toc.html. We briefly describe them here. The CM and CE cards specify comments. The GW cards specify the geometry of the wires with a wire label, a number of segments, the X, Y, Z positions of the wire ends, and finally a wire diameter. All dimensions are in meters. The GE card specifies the end of the geometry input. The LD cards specify the conductivity of each of the wire elements. The FR card specifies the frequency used to

[1]Paul.Ray@nrl.navy.mil

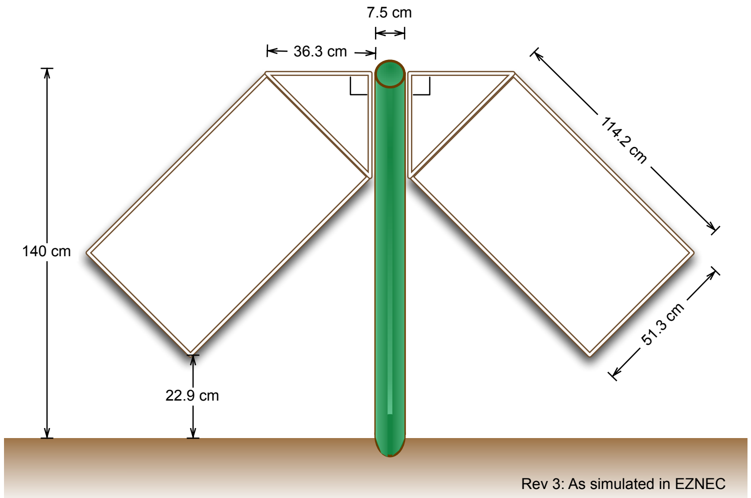

Fig. 1.— Simplified schematic of a GASE dipole and mast. Only one polarization is shown and supporting cross bar is left off for clarity. The measurements are as simulated in the EZNEC simulation. Some of the measurements are slightly different than as measured on the production version.

Fig. 2.— Photograph of GASE dipole installed at the Haystack Observatory site.

stimulate the antenna. The GN card specifies the properties of the ground plane. The EX card specifies where and how to excite the antenna. Finally, the RP card specifies how the radiation pattern is to be sampled in the output. Note that the balun input impedance is not specified in the input file because it is not used by NEC in the calculation.

3.1. Impedance

The EZNEC simulations also allow us to calculate the feedpoint impedance as a function of frequency. This is displayed as a simple cartesian plot and a standard Smith chart in Figure 3.

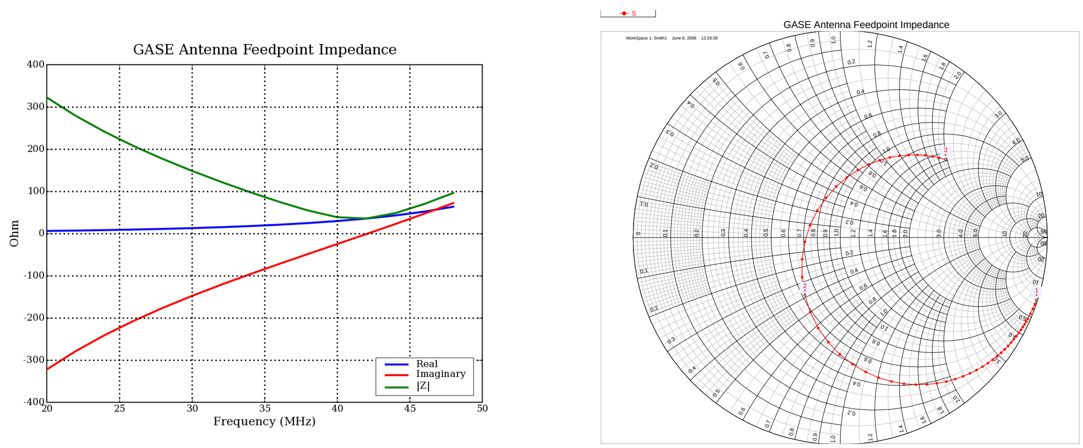

Fig. 3.— *Left:* Real part (R), imaginary part (reactance, X), and magnitude ($|Z|$) of the feedpoint impedance as a function of frequency. *Right:* GASE antenna Smith Chart over a frequency range of 20–50 MHz. Note that the Smith chart is normalized to a 50 Ω input impedance for the balun, which is off by a factor of two from the actual balun input impedance.

3.2. Dipole Response Pattern

The dipole response pattern results are plotted in Figures 4–7.

Listing 1 Listing of EZNEC input file

```
CM GASE Dipole
CE
GW 1,3,.03742,0.,1.4,.4004345,0.,1.4,.0047625
GW 2,3,.03742,0.,1.4,.03742,0.,1.036986,.0047625
GW 3,4,.4004345,0.,1.4,.03742,0.,1.036986,.0047625
GW 4,8,.4004345,0.,1.4,1.208283,0.,.5921519,.0047625
GW 5,8,.03742,0.,1.036986,.8452684,0.,.2291372,.0047625
GW 6,4,1.208283,0.,.5921519,.8452684,0.,.2291372,.0047625
GW 7,1,.03742,0.,1.4,-.03742,0.,1.4,.0047625
GW 8,3,-.03742,0.,1.4,-.4004345,0.,1.4,.0047625
GW 9,3,-.03742,0.,1.4,-.03742,0.,1.036986,.0047625
GW 10,4,-.4004345,0.,1.4,-.03742,0.,1.036986,.0047625
GW 11,8,-.4004345,0.,1.4,-1.208283,0.,.5921519,.0047625
GW 12,8,-.03742,0.,1.036986,-.8452684,0.,.2291372,.0047625
GW 13,4,-1.208283,0.,.5921519,-.8452684,0.,.2291372,.0047625
GE 1
LD 5,1,0,0,5.7471E+7,1.
LD 5,2,0,0,5.7471E+7,1.
LD 5,3,0,0,5.7471E+7,1.
LD 5,4,0,0,5.7471E+7,1.
LD 5,5,0,0,5.7471E+7,1.
LD 5,6,0,0,5.7471E+7,1.
LD 5,7,0,0,5.7471E+7,1.
LD 5,8,0,0,5.7471E+7,1.
LD 5,9,0,0,5.7471E+7,1.
LD 5,10,0,0,5.7471E+7,1.
LD 5,11,0,0,5.7471E+7,1.
LD 5,12,0,0,5.7471E+7,1.
LD 5,13,0,0,5.7471E+7,1.
FR 0,1,0,0,50.
GN 2,0,0,0,13.,.005
EX 0,7,1,0,1.414214,0.
RP 0,19,73,1001,0.,0.,5.,5.,0.
EN
```

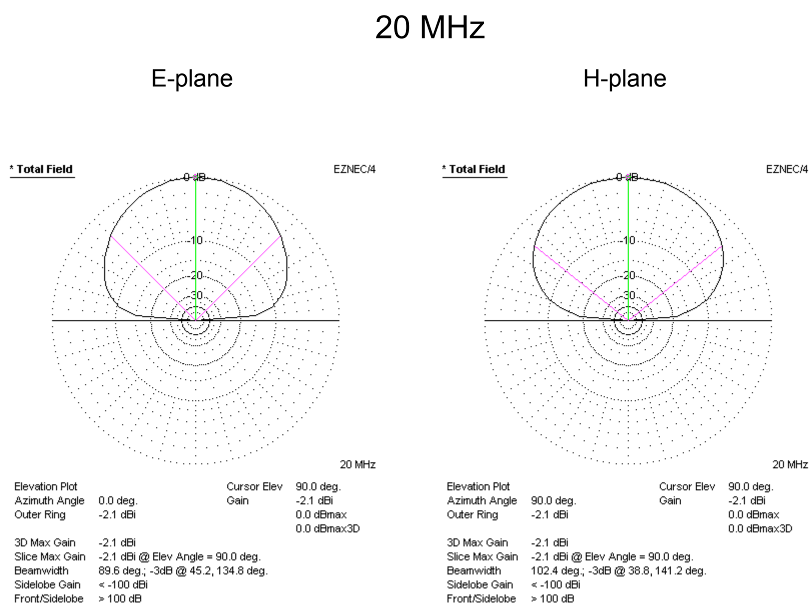

Fig. 4.— GASE dipole pattern at 20 MHz

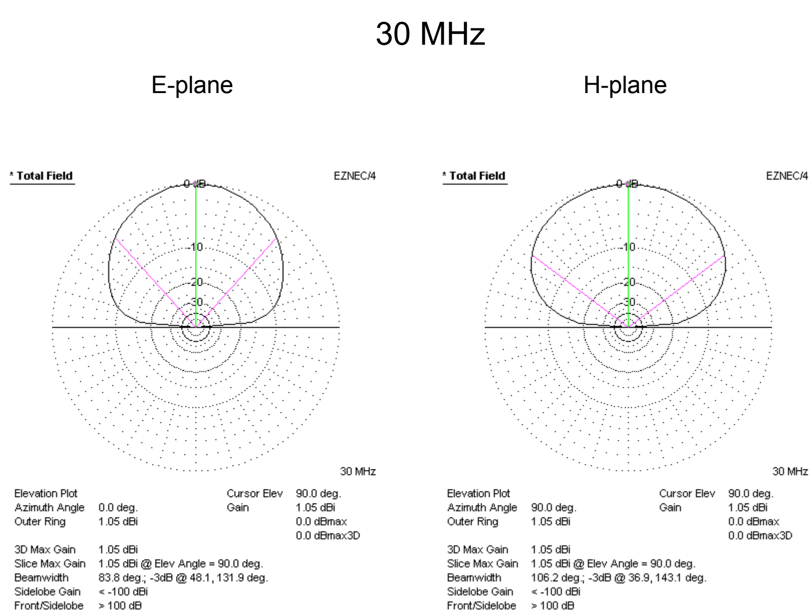

Fig. 5.— GASE dipole pattern at 30 MHz

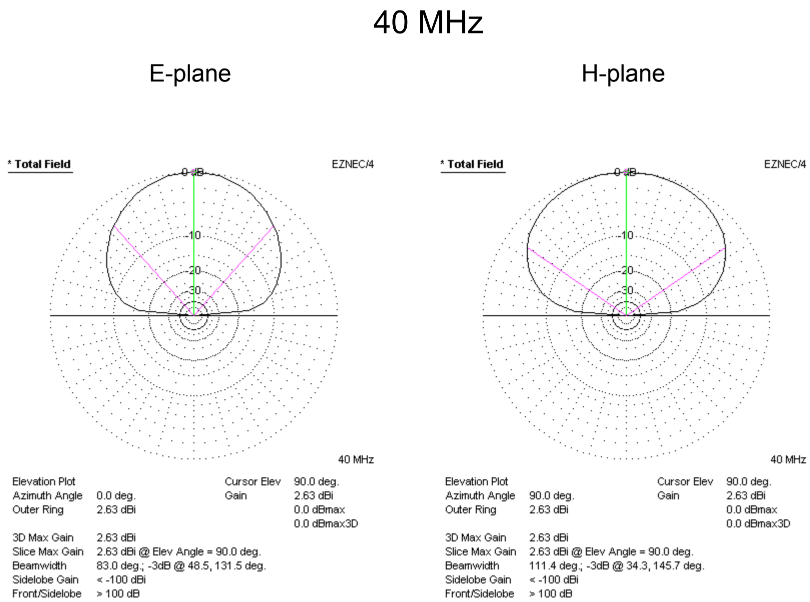

Fig. 6.— GASE dipole pattern at 40 MHz

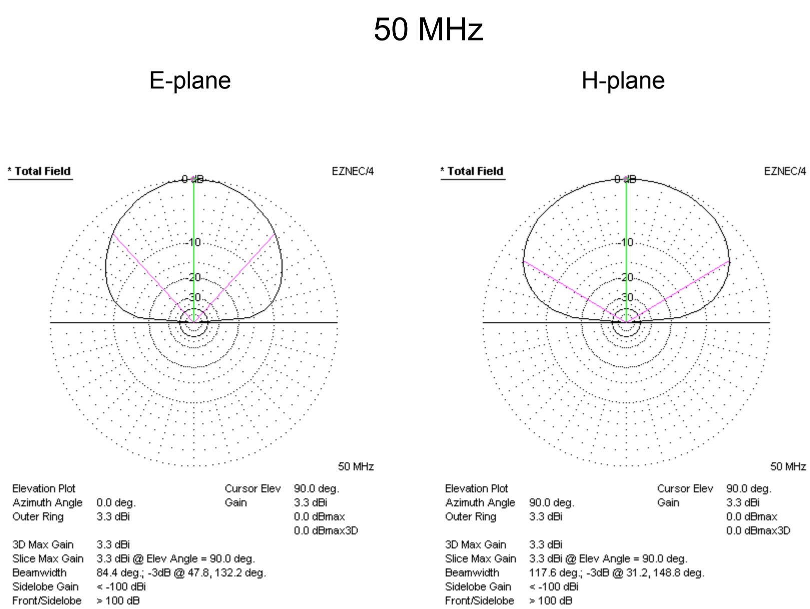

Fig. 7.— GASE dipole pattern at 50 MHz

3.3. Sky Noise Response

To understand the performance of the antenna for astronomical observations we need to understand the response to sky noise. The ideal scenario is one in which the effective noise temperature ($T_{\rm sys}$) of the system is dominated by the effective sky temperature corresponding to the Galactic noise spectrum,

$$T_{\rm sky} = \frac{I_\nu c^2}{2k\nu^2}, \tag{1}$$

where $k = 1.38 \times 10^{38}$ J/K is Boltzmann's constant, c is the speed of light, ν is the frequency in Hz, and I_ν is the intensity of the Galactic noise in W m^{-2} Hz^{-1} sr^{-1}. Following Ellingson (2005) and Cane (1979), we adopt the following approximation for I_ν,

$$I_\nu \approx I_{\rm g}\nu^{-0.52} + I_{\rm eg}\nu^{-0.80}, \tag{2}$$

where $I_{\rm g} = 2.48 \times 10^{-20}$ and $I_{\rm eg} = 1.06 \times 10^{-20}$. The resulting $T_{\rm sky}$ over the GASE frequency range is plotted in Figure 8

Although the temperature presented to the antenna is well modeled as $T_{\rm sky}$, this is not the effective temperature that will be observed by the actual system. This is primarily a result of two effects: (1) the mismatch between the antenna feedpoint impedance and the balun input impedance, and (2) losses due to the finite ground conductivity (the finite conductivity of the copper antenna wires can safely be ignored). An analysis of these effects is presented in detail by Ellingson (2005), and we will just summarize the relevant results here.

The "impedance mismatch efficiency", $1-|\Gamma|^2$, is the fraction of power available at the antenna that is effectively coupled into the preamplifier, where Γ is the voltage reflection coefficient defined as,

$$\Gamma = \frac{Z_{\rm pre} - Z_{\rm a}}{Z_{\rm pre} + Z_{\rm a}}, \tag{3}$$

which is plotted in Figure 9.

A related quantity, the "voltage standing wave ratio" (VSWR) is also often used to characterize this impedance mismatch, and is defined as

$$\mathrm{VSWR} = \frac{1+|\Gamma|}{1-|\Gamma|}. \tag{4}$$

The VSWR is plotted in Figure 10.

The ground losses are characterized by an efficiency, e_r, which is 1.0 for a perfect electric conductor (PEC) ground. Over a real ground, e_r will be frequency dependent. Approximate ground losses can be calculated by comparing the total gain of the antenna in an EZNEC simulation run with a PEC ground to one run with real ground properties. The difference between these two gains is presumed to be the ground loss. This ground loss factor is plotted in Figure 11

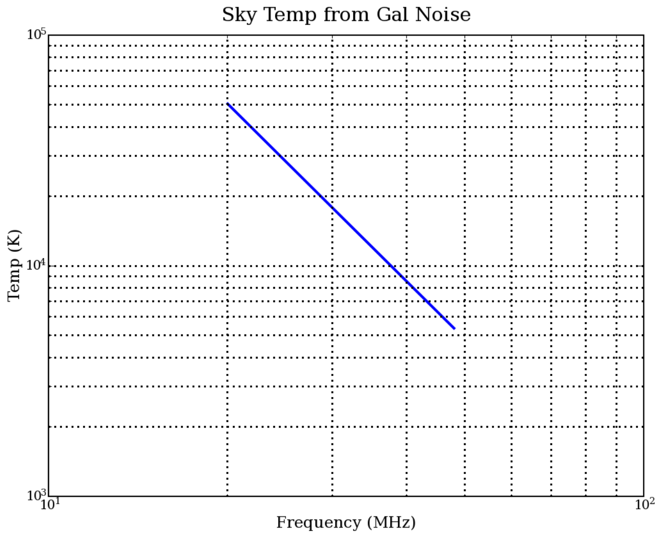

Fig. 8.— $T_{\rm sky}$ over the GASE frequency range.

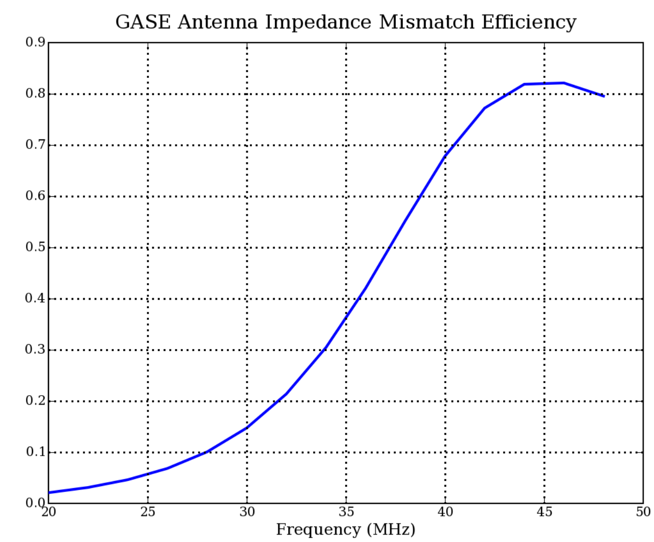

Fig. 9.— GASE antenna impedance mismatch efficiency $(1 - |\Gamma|^2)$ vs. frequency.

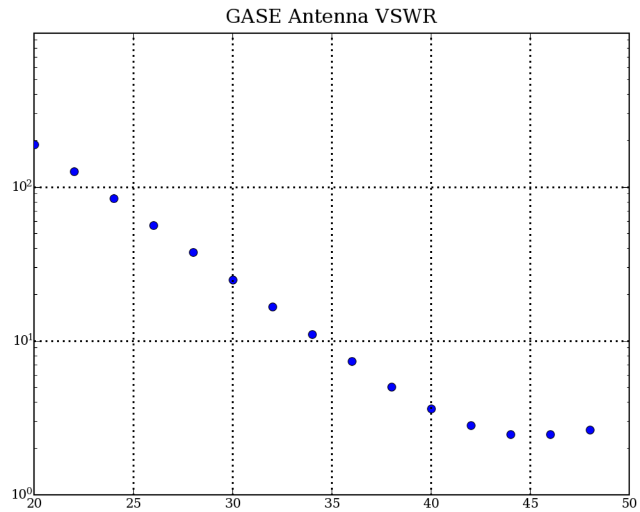

Fig. 10.— GASE antenna standing wave ratio (SWR) vs. frequency.

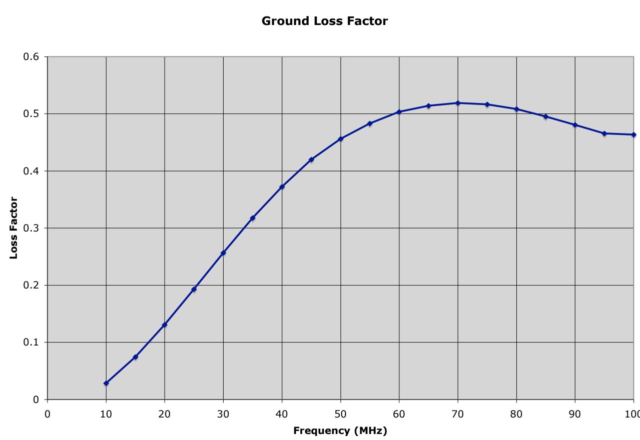

Fig. 11.— Ground loss, e_r as a function of frequency..

Combining the impedance mismatch inefficiency and ground losses yields an observed antenna temperature,

$$T_{\rm ant} = e_r(1 - |\Gamma|^2)T_{\rm sky}. \tag{5}$$

This observed temperature is plotted in Figure 12

3.4. Diurnal Sky Noise Variation

The previous analysis assumed a constant Galactic sky noise appropriate for the Galactic pole region. In reality, of course, the effective sky temperature as the Galactic center and plane rotate overhead. To simulate this effect, we modeled the sky temperature distribution using the 408 MHz all sky map from Haslam et al. (1982), scaled to 34 MHz using a spectral index of 2.55. This map was convolved with the antenna pattern calculated using EZNEC at 30 MHz (for the "Large Blade" antenna, which should be rather close to the GASE dipole pattern), at an assumed latitude of 42.4° North, and for typical ground properties as specified above. The resultant plot of $T_{\rm sky}$ vs. local sidereal time (LST) is shown in Figure 13.

4. Active Balun

The active balun can be simply characterized by the parameters in Table 1.

Table 1. Active balun (preamplifier) specifications

Specification	Value
Polarization	Single
Gain	$G = +24$ dB
Input Impedance	$Z_{\rm pre} = 100\ \Omega$ ($50\ \Omega$ per arm)
Noise Figure	NF = 2.7 dB ($T_{\rm pre} = 250$ K)
Linearity (3rd order intercept)	IIP3 = 7.5 dBm
Output Impedance	$Z_{\rm out} = 50\ \Omega$

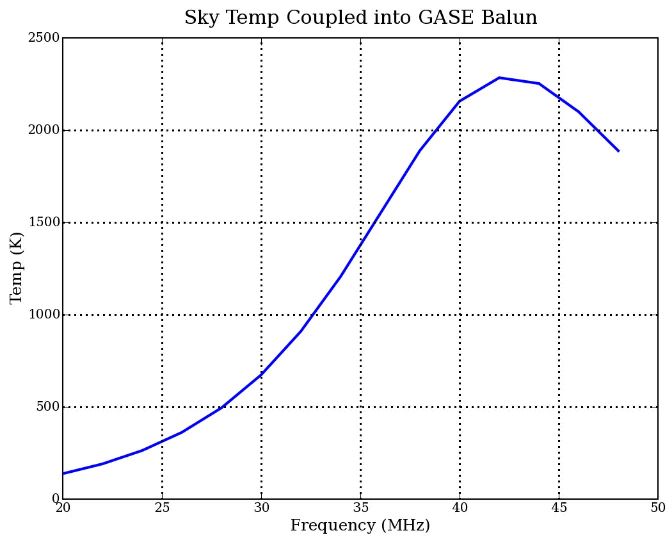

Fig. 12.— Antenna temperature predicted to be observed by GASE, assuming the ground loss e_r as in Figure 11, $1 - |\Gamma|^2$ as in Figure 9, and $T_{\rm sky}$ as in Figure 8.

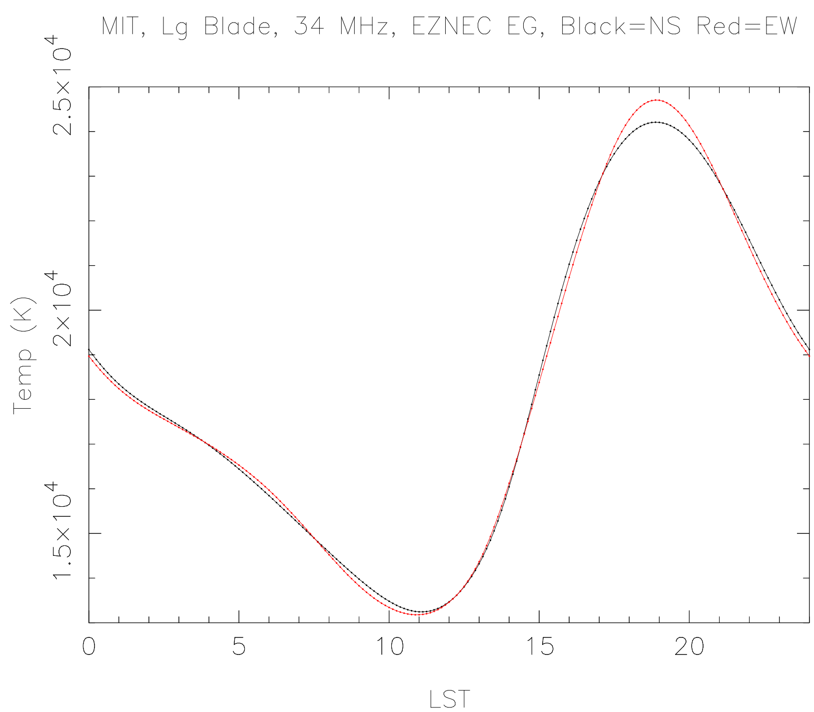

Fig. 13.— Simulated sky temperature at 34 MHz vs. LST for the GASE site and aproximate antenna pattern (black = dipole oriented N-S, red = dipole oriented E-W). This is the time-dependent $T_{\rm sky}$ and does not include the effects of ground loss or impedance mismatch efficiency.

REFERENCES

Cane, H. V. "Spectra of the nonthermal radio radiation from the galactic polar regions," MNRAS, **189**, 465 (1979)

Ellingson, S. W., "Antennas for the Next Generation of Low-Frequency Radio Telescopes", IEEE Transactions on Antennas and Propagation, **53**(8), 2480 (2005)

Haslam, Stoffel, Salter & Wilson, "A 408 MHz All-Sky Continuum Survey. II. The Atlas of Contour Maps", A&AS, **47**, 1 (1982)

Morales, M. F., Hewitt, J. N., Kasper, J. C., Lane, B., Bowman, J., Ray, P. S., & Cappallo, R. J. 2006, Astronomical Society of the Pacific Conference Series, **345**, 512

This preprint was prepared with the AAS LaTeX macros v5.2.